January 2014

Ir Laser-induced Perturbations Of The Voltage-dependent Solute Carrier Protein, Slc26a5

Oluwarotimi Nettey

IR Laser-induced perturbations of the voltage-dependent solute carrier protein, SLC26a5.

A Thesis Submitted to the
Yale University School of Medicine
In Partial Fulfillment of the Requirements for the
Degrees of Doctor of Medicine
And
Master of Health Science
By

Oluwarotimi Sewedo Nettey
2014

Acknowledgments

This research was supported by a Howard Hughes Medical Institute Medical Research Fellowship to Oluwarotimi Nettey. I am indebted Joseph Santos-Sacchi who not only provided me with this wonderful and atypical opportunity but also encouraged and instructed me amidst the various challenges of patch clamping. Many thanks to Lei Song, PhD and Jun-Ping Bai, PhD who provided the direction and technical expertise for my project and kept my level of enthusiasm high. To my parents and husband, your support and encouragement are highly valued. Thank you for taking the walk with me and helping me see the entire process through.

Table of Contents

IR LASER-INDUCED PERTURBATIONS OF THE VOLTAGE-DEPENDENT SOLUTE CARRIER PROTEIN, SLC26A5. Oluwarotimi S. Nettey and Joseph Santos-Sacchi. Sections of Otolaryngology and Neurobiology, Department of Surgery, Yale University, School of Medicine, New Haven, CT.

Alterations in membrane capacitance can arise from linear and nonlinear sources. For example, changes in membrane surface area or dielectric properties can modify capacitance linearly, whereas sensor residues of voltage-dependent proteins can modify capacitance nonlinearly. Here, we examined the effects of fast temperature jumps induced by an IR laser in control and prestin (SLC26a5)-transfected HEK cells under whole cell voltage clamp. Prestin's voltage sensor imparts a characteristic bell-shaped, voltage-dependent nonlinear capacitance (NLC). Temperature jumps in control HEK cells cause a monophasic increase in membrane capacitance (C_m) regardless of holding voltage due to double layer effects. Prestin-transfected HEK cells, however, additionally show a biphasic increase/decrease in C_m with a reversal potential corresponding to the voltage at peak NLC of prestin (V_h), attributable to a rapid temperature-following shift in V_h, with shift rates up to 14 V/s over the course of a 5 ms IR pulse. Treatment with salicylate, a known inhibitor of NLC, re-establishes control cell behavior. A simple kinetic model recapitulates our biophysical observations. These results verify a voltage-dependent protein's ability to respond to fast temperature perturbations on par with double layer susceptibility, likely arising from prestin's unique ability to move sensor charge at kilohertz rates, a requirement for the OHC's role as cochlear amplifier.

Introduction

The interaction of various hair cell types within the organ of Corti, an anatomically inaccessible structure within the inner ear, drives the processing and amplification of sound in mammals. Outer hair cells (OHCs) are mechanically robust units of the inner ear with both sensor and effector properties[1,2]. They rapidly and reversibly deform in response to sound vibrations entering through the middle ear, which they detect as transient fluxes in membrane potential[3]. Electrical stimulation of OHCs was first observed to result in twitching of hair cells in vitro by Brownell in 1985[3,4], with length changes in the outer hair cells occurring in kilohertz ranges[5-8]. These rapid mechanical changes are thought to drive the boost in hearing, which mammals experience near threshold levels, and form the basis of cochlear amplification[1].

Cochlear amplification denotes a process whereby responses to low level acoustic stimuli are enhanced, resulting in an increase in auditory sensitivity and frequency resolving power. Rapidly contracting and elongating OHCs feed impinging mechanical energy back into the cochlea resulting in a boost in stimulation to the inner hair cells, the effector cells for neurotransmission to the auditory cortex. These mechanical changes are postulated to result from conformational transitions in the integral lateral membrane motor proteins, which affect membrane surface area and resultant capacitance[9-12]. Prestin motor units (SLC26a5), proteins of the SLC26 anion transporter family[13], are localized to the OHC lateral membrane, drive rapid mechanical changes in OHCs and are associated with a nonlinear capacitance (NLC).

NLC is a displacement or gating current[14], which arises as the first derivative of a two-state Boltzmann function relating prestin voltage-sensor charge as a function of transmembrane voltage. The displacement current is sigmoidal in shape and highly voltage dependent[5,15-20]. NLC reflects the movement of charged residues within these prestin motor units and peaks at a voltage (V_h) where OHC mechanical response is maximally sensitive to voltage. NLC is thought to be the electrical correlate of voltage dependent conformational changes within the prestin motor protein and serves as the electric signature for the motile response of outer hair cells. Nonlinear capacitive current is exquisitely vulnerable to perturbations in biophysical forces including membrane tension[19], resting potential[14,21] and temperature[22,23], which subsequently affect frequency selectivity and sound amplification[17-19,22-24]. Specifically, rapid increases in intracellular pressure, negative holding potential, and temperature shift the nonlinear capacitance function in a depolarizing direction along the voltage axis in a multi-exponential time-dependent manner.

Evidence for voltage-dependent mechanical activity has been observed in human embryonic kidney cells (HEK cells) transfected with prestin. Recordings of these cells show a motile response and generation of mechanical force in response to electrical stimulation much like outer hair cells[14]. Mice knockouts of prestin, a member of the SL26 anion transporter family[13], similarly show a loss of motile response in isolated outer hair cells in addition to a 40- to 60-dB reduction in cochlear sensitivity[25,26], thereby demonstrating that prestin is responsible for the electromotile response of OHCs. Temperature dependent effects on nonlinear capacitive current

have also been successfully replicated in prestin-transfected non-auditory cells[24]. Of note, mutations of human *Pres,* the gene responsible for prestin, have been linked to the development of non-syndromic congenital, bilateral hearing loss in infants. Much work needs to be done to better understand how mutations in prestin and its various interactions result in hearing loss.

Here we examine the effects of fast temperature jumps induced by an infrared laser in control and prestin-transfected HEK293 cells under whole cell voltage clamp conditions. Many proteins have a strong temperature dependence, which may in turn modulate their function[27]. Temperature effects on protein kinetics range from modulating ion conductance, voltage sensitivity, to changing rates of channel opening and inactivation through a host of metabolic processes [28-31]. Previous studies also show that temperature can gate channel response by changing the activation energy required for protein conformational change[28,32]. Bezanilla et al found that rapid temperature jumps altered linear membrane capacitance in a reversible manner giving rise to depolarizing currents that likely resulted from the movement of charged particles that were previously distributed asymmetrically across the resting cell membrane[28,33].

Here we show that both linear and prestin derived nonlinear capacitive currents are sensitive to fast temperature jumps. Whereas, fast temperature jumps monotonically increase linear C_m in a voltage- independent manner as previously reported[28], the Boltzmann distribution of motors along the voltage axis is rapidly and simultaneously altered in a reversible manner. Prestin derived nonlinear capacitive

effects vary according to the cell's holding potential and furthermore show reversal in polarity at membrane potentials near the peak voltage of nonlinear capacitance. Our observations clearly show that voltage-dependent proteins, given sufficiently fast kinetics as with prestin, can contribute to rapid alterations of membrane capacitance.

Hypothesis and Specific Aims

The sensitivity of prestin motor function to biophysical forces such as temperature and resting voltage has been characterized in detail in mammalian models of mature outer hair cells[15,24,34]. Several studies have determined that nonlinear capacitance and electromotile response can also be generated by prestin-transfected HEK cells[35]. The time course for the development of these sensitivities after prestin transfection however is unclear. Based on previous work in our lab, we know that the voltage **V**h corresponding to maximal nonlinear capacitance peaks approximately 30 hours after tetracycline induction in a prestin-transfected cell line[36], and should accordingly function like a mature outer hair cell.

We hypothesize that similarly to mature OHCs, temperature jumps in prestin-transfected HEK cells should shift the NLC function in a depolarizing direction over time. As a control experiment, known NLC inhibitors such as salicylate should yield an increase in the linear component of membrane capacitance only and the diminution of nonlinear capacitive currents in prestin-transfected HEK cells.

Relevance

All cells have linear capacitance based on membrane properties; particularly integral membrane proteins can increase surface area and are further enabled to store charge. Linear capacitance is sensitive to temperature effects through various mechanisms including thinning or modulation of viscosity of phospholipid bilayer as previously reported[28]. OHCs are unique because of their ability to generate nonlinear capacitive effects through the movement of charged prestin residues within the membrane bilayer. How temperature affects the generation and interaction of membrane nonlinear capacitive effects with its linear component is poorly understood. Our study aims to elucidate a key biophysical property, namely temperature, which underlies prestin's ability to undergo rapid conformational changes.

Methods

Cell culture and expression

We previously developed a tetracycline-inducible HEK293 cell line that highly expresses prestin upon addition of a transduction agent[37]. HEK 293 cells were cultured in Dulbecco's modified Eagle's high glucose base medium (DMEM) containing 50 U/ml each of penicillin, streptomycin and L-Glutamine, supplemented with 10% fetal bovine serum, 5 ug/ml of blasticidin and 130 ug/ml of zeocin. The cells were maintained at 37°C in a humidified incubator gassed with 5% CO_2. The addition of 1μg/ml tetracycline to the growth medium induced prestin expression and trafficking to the cell membrane. Patch clamp recordings of the cells were made 24 to 72 hours after induction at room temperature.

Infrared laser

Photonic stimulation with a Capella R-1850 laser was used to deliver rapid temperature jumps to cells in the recording chamber. The laser was coupled to a 600 µm diameter optical fiber which delivered an output wavelength of 1850 nm in pulses of variable duration. At a power setting of 100%, optical pulse energy was 5 mJ/ms. Laser stimulation was computer-controlled via TTL, and synchronized to voltage clamp commands using an Axon Instruments 1320 series A/D and D/A board. The laser fiber was mounted on a micromanipulator, and the tip was placed within 0.5 mm of the recorded cell, ensuring that the whole cell was irradiated. Constant temperature jumps were applied to the surface of each cell after a gigohm seal was formed with the recording electrode. **Figure 1** shows a view of the recording chamber as seen from the recording microscope.

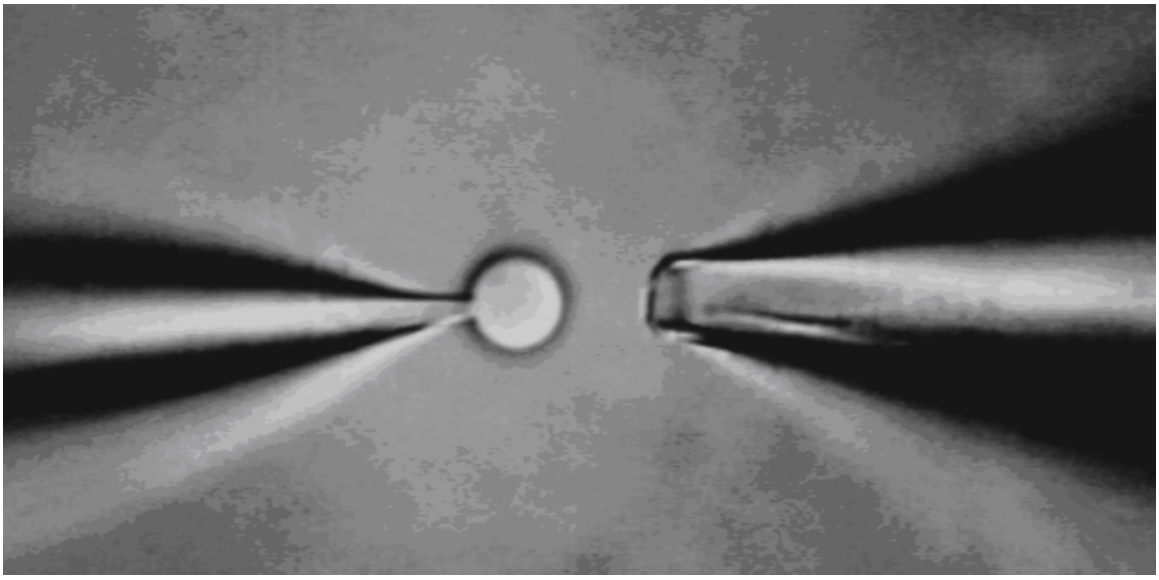

Figure 1 A view of the recording chamber showing the laser-electrode configuration during cell recording. The recording electrode is continuous with the surface of the cell membrane. The laser tip is proximal enough to successfully irradiate the whole cell.

We assume that our observations arise from temperature changes within the membrane fostered by temperature changes in bath solution water, similar to conclusions made by others[27,28]. We calibrated the temperature change indirectly by monitoring changes in patch electrode resistance (R_S), i.e., changes in I_{RS} with fixed voltage stimulation, as those investigators did. Thus, in preliminary experiments, we correlated R_S vs. changes in whole bath temperature. In the physiological experiments, our admittance analysis of currents allows us to quantify R_S changes independent of C_m and R_m changes[38]. We found that a 33% change in R_S indicates a temperature change of 17^oC. In our experiment, peak R_S change averaged 31.2 +/- 0.02 % (n=5) at 40 % laser power. Our previous observation that a 20 mV shift in NLC V_h occurs per 10^oC change in bath temperature provides corroboration of these estimates[23,24].

Patch clamp electrophysiology

Ionic blocking solutions were used to remove voltage-dependent ionic conductances so that capacitive currents could be analyzed in isolation. Extracellular bath solutions for whole-cell recording in HEK293 cells consisted of (mM): 20 TEA, 20 CsCl, 2 $CoCl_2$, 1 $MgCl_2$, 10 Hepes, 1 $CaCl_2$, 100 NaCl adjusted to pH 7.22 with NaOH and 301 mOsm using D-glucose. An extracellular perfusion solution containing 132 NaCl, 2 $CaCl_2$, 2 $MgCl_2$, 10 Hepes, 10 Na Salicylate (pH 7.20, 300 mOsm) was also used for experiments to block NLC. Electrodes were filled with (mM): 140 CsCl, 2

$MgCl_2$, 10 Hepes, 10 EGTA (pHm7.27, 302 mOsm). All chemicals used were purchased from Sigma.

Borosilicate glass pipettes were pulled using a P-2000 laser-heating pipette puller (Sutter Instruments) to initial resistances ranging between 3.5-5 MΩ. Pipette stray capacitance was compensated prior to recording and voltages were corrected for effects of series resistance off line. A Nikon Eclipse TE300 inverted microscope with Hoffmann optics was used to observe the cells during electrical recording. Round, isolated cells growing on a glass cover slip were patched 24-72 hours after tetracycline induction.

Cells were clamped to a holding potential of 0 mV using an Axon 200B patch clamp amplifier. During the temperature jump protocol, cells were held under voltage clamp at 0 mV and stepped in 30 mV increments (from hyperpolarizing values of -150mV to 150mV) for 1024 ms during which a brief IR laser pulse was delivered to the cells for each voltage step. Solution exchange with salicylate was performed using gravity flow. All recordings were made at room temperature. Local temperature measurements of the cells were calculated by measuring changes in electrode resistance and extrapolating from a resistance-temperature calibration curve[27]. A resistance-temperature calibration curve was obtained by observing changes in pipette resistance in a hot bath solution (~55 °C) that was allowed to cool passively. Electrical conductivity is known to be linear over a large temperature range hence a linear calibration relationship was fitted to log (Resistance) versus 1/temperature. Resistance time courses during application of the infrared laser pulses were extracted and then

converted to temperature using the calibrated relationship.

Cell capacitance was measured under whole cell configuration using jClamp software (SciSoft, CT, USA; www.SciSoftCo.com). Voltage records sampled at 10 μs were filtered at 10 kHz with an 8 pole Bessel filter and saved to disk for off-line analysis. Nonlinear capacitance was measured using a continuous high resolution (2.56 ms sampling) two-sine stimulus protocol (10 mV peak at both 390.6 and 781.2 Hz) superimposed onto the voltage command[21,38]. Capacitance data were fit to the

$$C_m = Q_{\max}\frac{ze}{kT}\frac{b}{(1+b)^2} + C_{lin}, \qquad b = \exp\left(\frac{-ze\left(V_m - V_h\right)}{kT}\right)$$

Equation 1

first derivative of a two-state Boltzmann function[14], where Q_{max} is the maximum nonlinear charge moved, V_h is voltage at peak capacitance or equivalently, at half maximum charge transfer, V_m is membrane potential, z is valence, C_{lin} is linear membrane capacitance, e is electron charge, k is Boltzmann's constant, and T is absolute temperature. Justification for using steady state fits of prestin's charge movement at the 2.56 ms C_m measurement sampling rate is that the parameters are largely stable (z, Q_{max}), except for V_h, across time samples. ΔC_m is defined as the difference between pre-IR and post-IR maximal capacitance. Results are reported as mean +/- standard error.

Model

A kinetic model of SLC26a5 that we previously developed[39] was used to understand the biophysical data. The model was developed to account for a chloride-dependent disparity between NLC and electromotility V_h, requiring intermediate transitions much slower than either chloride or voltage-dependent transitions. A model cartoon is shown in Figure 5a of that reference[39].

$$X_o \underset{k_2}{\overset{k_1}{\rightleftharpoons}} X_c \underset{\beta_0}{\overset{\alpha_0}{\rightleftharpoons}} X \underset{\beta}{\overset{\alpha}{\rightleftharpoons}} C$$

Equation 2

The model has very fast anion (chloride) binding and unbinding transitions ($X_O \leftrightarrow X_C$) and very fast voltage-dependent conformational transitions ($X \leftrightarrow C$). The transition to state ***C*** carries a unit charge, q; Q_{max}, total charge moved, will reflect the maximal accumulation of motors in that state. Nestled between the anion-binding and voltage-dependent transitions, resides a non-voltage- dependent transition ($X_C \leftrightarrow X$), which is very much slower than the other two transitions.

The kinetic model was assessed using Matlab Simulink via an automation link with jClamp (www.scisoftco.com). The kinetic model was interfaced to jClamp via a model of the patch clamp amplifier and cell. The linear component of the patch-cell model possessed an R_S of 5 MW, R_m of 500 MW and C_{lin} of 10 pF. The nonlinear component, NLC, derived from charge movement of the SLC26a5 model, parameters being $k_1=10^7 * [Cl]_{in}$, $k_2=10^7 * k_d$, $\alpha_0=75 * \exp(t_m)$, $\beta_0=95$, $\alpha=10^6 *$

$\exp(zFV_m/2RT)$, $\beta=583 * 10^9 * \exp(-zFV_m/2RT + t_m/2 - E_a/RT)$, $k_{d\ Cl}$ =0.001,T=296 kelvin, E_a=45 kJ/mol, F=9.648 * 10^4 C/mol, R=8.315 J/Kmol, k=1.381 * 10^{-23} VC/K.

The rates α_0 and β are tension sensitive, since tension is known to increase prestin residence in the expanded (X) state (5, 6), t_m in units kT (eRT/F); the rate β is temperature sensitive, with Arrhenius activation energy, E_a. α and β are voltage-dependent, with sensor valence *z=0.7*. At *T*= 296 kelvin, V_m= 0 mV, T_m = 0 kT, and $[Cl]_{in}$ = 0.14 M, *initial rates are* k_1*=1.4e6,* k_2*=1e4,* α_0*=75,* β_0*=95,* α*=1e6, and* β*=1e5.*

Results

Capacitance

The rapid temperature change associated with an IR laser pulse delivered directly to a cell via optical fiber alters membrane capacitance. Control HEK cells and cells of our un-induced SLC26a5 HEK cell line increase their linear membrane capacitance in a voltage-independent fashion. **Figure 2a** shows C_m measures of a voltage clamped, un-induced SLC26a5 HEK cell for a wide range of holding potentials.

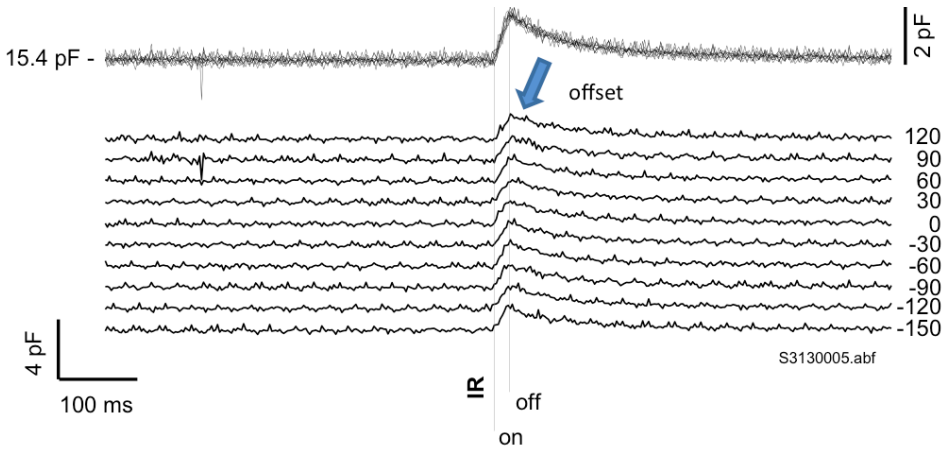

Figure 1a IR laser-induced temperature jump alters linear capacitance. Under whole cell voltage clamp, an un-induced SLC26a5 HEK cell was nominally stepped to the membrane potentials indicated. During the voltage step an IR laser pulse of 20 ms duration was delivered via optical fiber. Regardless of holding potential, the laser

The delivery of a 20 ms IR pulse (at 40% of maximal laser power) induces a linearly ramped increase in C_m coinciding with the duration of the pulse. In order to better visualize the overlapped traces and indicate holding voltage, we offset the traces by an arbitrary constant, allowing clearer observation of the voltage-independence. The increase in C_m is 10.8 +/-2.5 % (n=5) of whole cell capacitance for a 20 ms pulse. In **Fig. 2a**, at laser offset, a single exponential decrease in C_m occurs with a time constant of 70 ms at 0 holding potential (81.5 +/- 3.2 ms; n=5). These linear and exponential phases of C_m change correspond, respectively, to a linear increase in temperature during the pulse and an exponential cooling of the bath solution/cytoplasm following the pulse, both reflected in simultaneous changes in series resistance of the pipette electrode (**Fig. 2b**). Our admittance analysis allows us to quantify R_S changes, which are known to correspond to temperature manipulations[27].

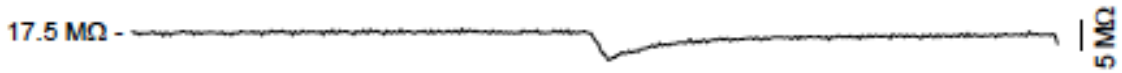

Figure 2b Series resistance simultaneously measured indicating a linear increase in temperature during the pulse, and an exponential cooling of bath media following the pulse

Figure 2c shows that increase in pulse durations induce increasing temperature changes that evoke larger C_m responses. Within our exposure range, we do not see any threshold effect for cell damage that is not associated with loss of cell recording.

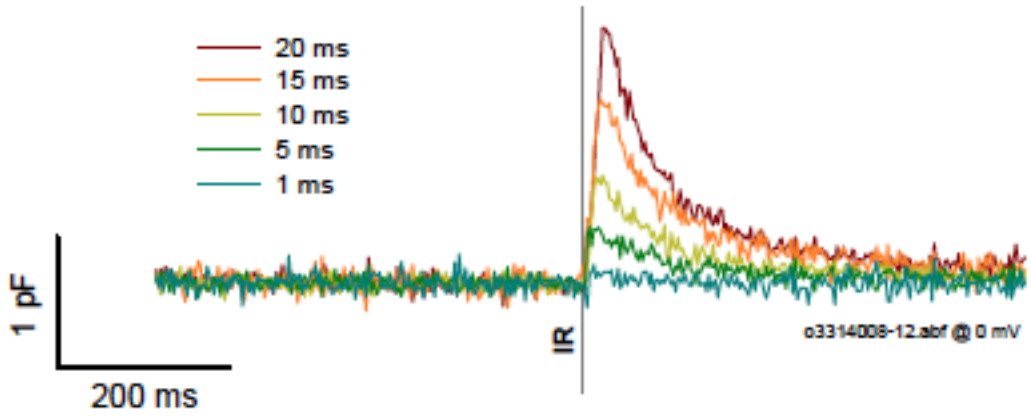

Figure 2c An increase in duration of the pulse results in a greater C_m change. Holding potential is zero mV.

In our SLC26a5 HEK cell line following tetracycline-induction, cells possess a voltage-dependent nonlinear capacitance (NLC) atop their linear capacitance[3 6]. This arises from the voltage sensor activity underlying the protein's role in outer hair cell (OHC) electromotility[23,24]. **Figure 3** illustrates the voltage-dependent nature of the induced HEK cell's C_m, and the influence of temperature jumps on NLC and linear C_m.

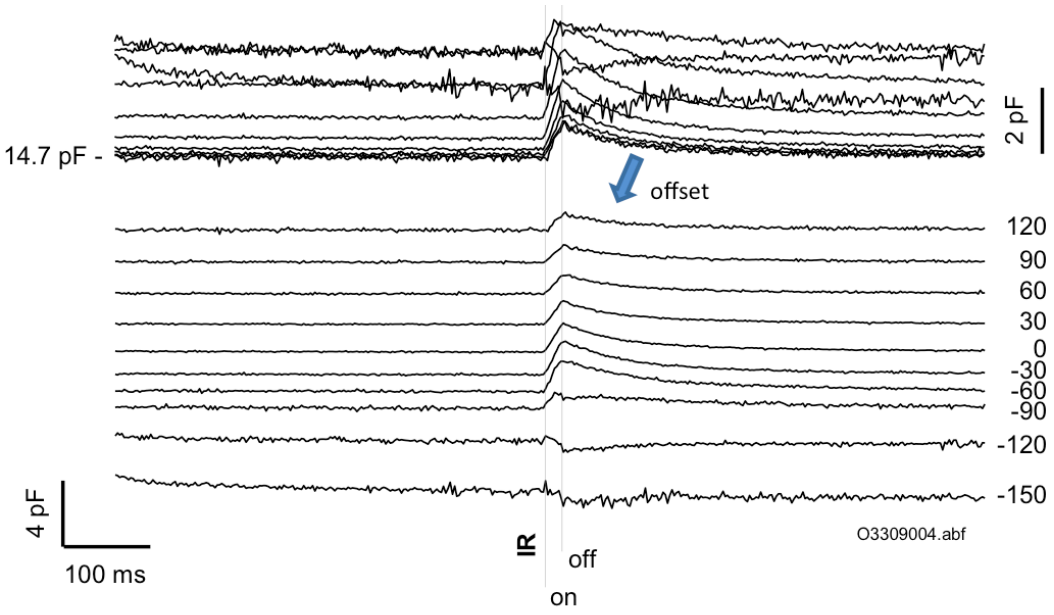

Figure 3 IR laser-induced temperature jump alters SLC26a5-generated nonlinear capacitance and linear capacitance. Under whole cell voltage clamp, an induced SLC26a5 HEK cell was nominally stepped to the membrane potentials indicated. During the voltage step an IR laser pulse of 20 ms duration (nominally 40 % Capella laser power) was delivered via optical fiber. The laser pulse induced a maximal change in C_m that depended on holding potential. The change could be either an increase or decrease.

Again, we offset the overlapped traces by an arbitrary constant, allowing clearer observation of the effects of IR pulse on C_m; obvious differences are found in comparison to un-induced HEK cells (see **Fig. 2**). Indeed, a voltage-dependent effect is now observed. In **Figure 3b**, C_m-V_m functions are plotted at various time points relative to the start of the IR pulse. The laser pulse induced a shift of the C_m-V_m

relation in the depolarizing direction. Following correction of voltages for R_S effects, Boltzmann fits to the data (see Methods) provide high resolution (2.56 ms) inspection of dynamic changes in NLC and linear capacitance during and after IR pulse (**Fig. 3c**).

In this example, NLC V_h shifted 40 mV in 20 ms at a linear rate of 2.03 V/s (average is 2.32 +/- 0.21 V/s; n=6) during the heating phase, and recovers (with temperature) exponentially with a time constant of 73 ms (average is 65.4 +/- 10.8 ms; n=6) during the cooling phase. The shift in V_h represents a redistribution prestin motors into the expanded conformation during heating. We have previously observed this shift over the course of minutes using Peltier control of bath solution temperature, the shift averaging about 20 mV/10^{o}C [23, 24]. In an additional two cells, we

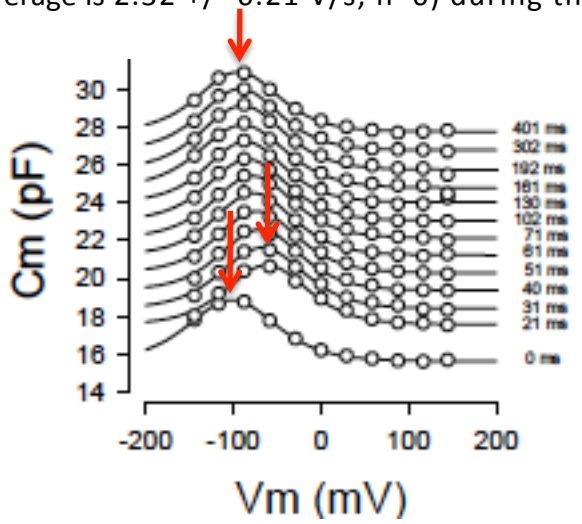

Figure 3b C_m-V_m plots of NLC as a function of time following pulse onset. Note the effect on the voltage- dependence of NLC, namely a shift to the right

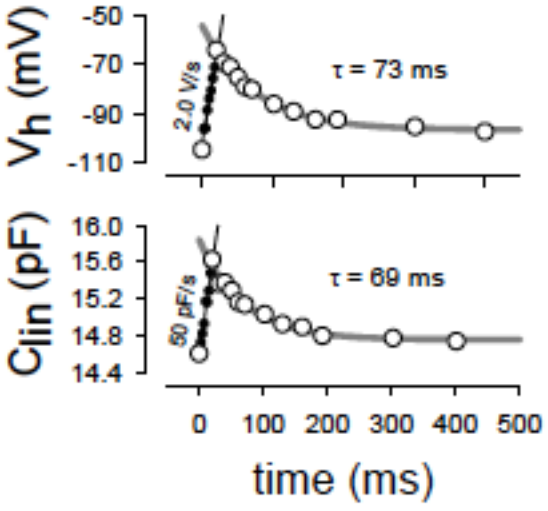

Figure 3c Changes in V_h and C_{lin} follow temperature. Rapid shifts and increases in C_{lin} occur during laser heating, and return back to initial levels during bath cooling.

were able to determine V_h shift with 5ms pulses at 90% laser power. The shift was 67 and 70 mV in 5ms or 13.4 and 14 V/s, indicating that heating rates and corresponding V_h shift rates increase with greater laser power. The increase in rates with laser power indicates that we have yet to observe the fastest response and are limited by laser power (we avoid higher than 90% power usage for technical reasons). Linear capacitance also changes simultaneously, with a similar time course to that of NLC V_h.

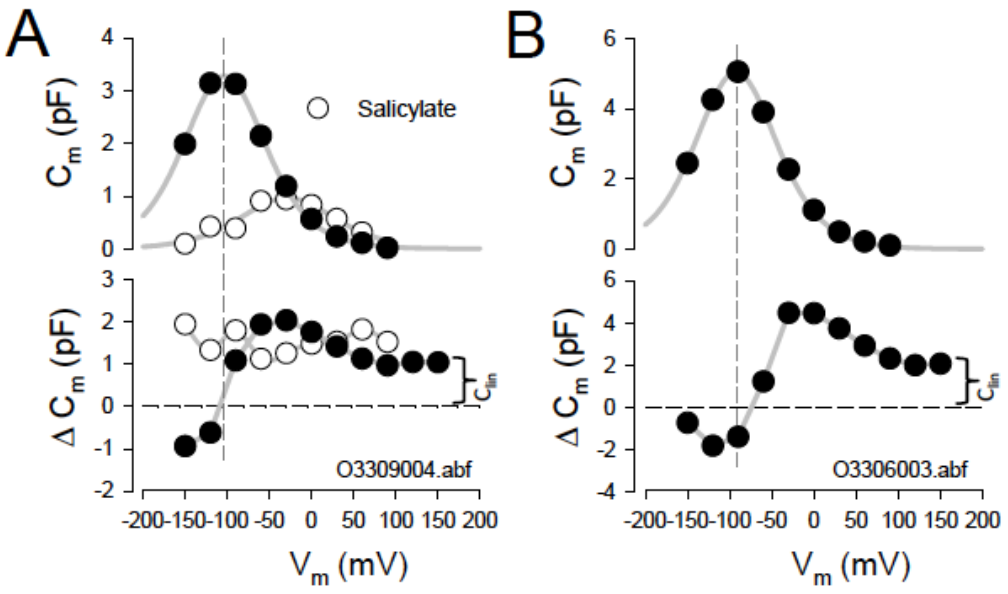

Figure 4 IR laser-induced temperature jump alters nonlinear capacitance showing increases and decreases, which reverse near V_h of NLC. Plotted NLC is that prior to temperature jump. Shown are data from two cells (A, B). ΔC_m at positive voltages remains offset from zero due to the temperature- dependent increase in linear C_m (curly brackets). In the first case (A), following data collection, salicylate (10 mM) was perfused onto the cell and collection was repeated. Salicylate removes the ΔC_m reversal as a result of NLC block, leaving intact a constant linear C_m increase across holding voltage. Averages are given in Results section.

In this case, there is a linear change of 50 pF/s during heating and a recovery due to cooling with a time constant of 69 ms (average is 78.9 +/- 7.7. ms; n=6). The changes due to cooling in linear capacitance are similar to those in control HEK cells. These rapid rates of change during heating and cooling mirror those changes in

temperature as gauged from R_S inspection or predicted from previous observations on temperature-dependent shifts of V_h during slow bath changes in temperature[23, 24], namely they correspond to a temperature induced change of 20 mV/ 10 ^{O}C. The difference in susceptibility of NLC and linear C_m to temperature jump is readily illustrated by the behavior of ΔC_m, defined as the maximal difference between pre-IR and post-IR capacitance. Examples from two cells are shown in **Figure 4a** and **b**. Whereas IR pulse-induced linear C_m changes occur at the same magnitude and direction (increase) regardless of holding potential (**Fig. 2**), NLC changes vary depending on holding potential, and reverse in direction near voltages (average is -96.8 +/- 6.4 mV; n=5) around NLC V_h (average is -94.7+/-6.2 mV; n=5), with an R^2 value of 0.9943 (**Fig. 4a, b**).Thus, it is possible, depending on the magnitude of NLC and its V_h (re holding potential), to induce a decrease in C_m by IR laser pulse. The effect of salicylate (10 mM) is not only to reduce NLC, as expected[40,41], but to eliminate the characteristic reversal of ΔC_m normally afforded by SLC26a5 expression, essentially returning the induced HEK cell back to its pre-induced condition (n=2). That is, only an increase in C_m is observed regardless of holding potential (**Fig. 4a**). To understand the data, we evaluate the temperature dependent behavior of a recently developed kinetic model of SLC26a5[39]. In the simulation, we simply modeled the temperature change as that revealed by our experimental measures of R_S; in this case, with a 23 ^{O}C maximum change (**Fig. 5a**).

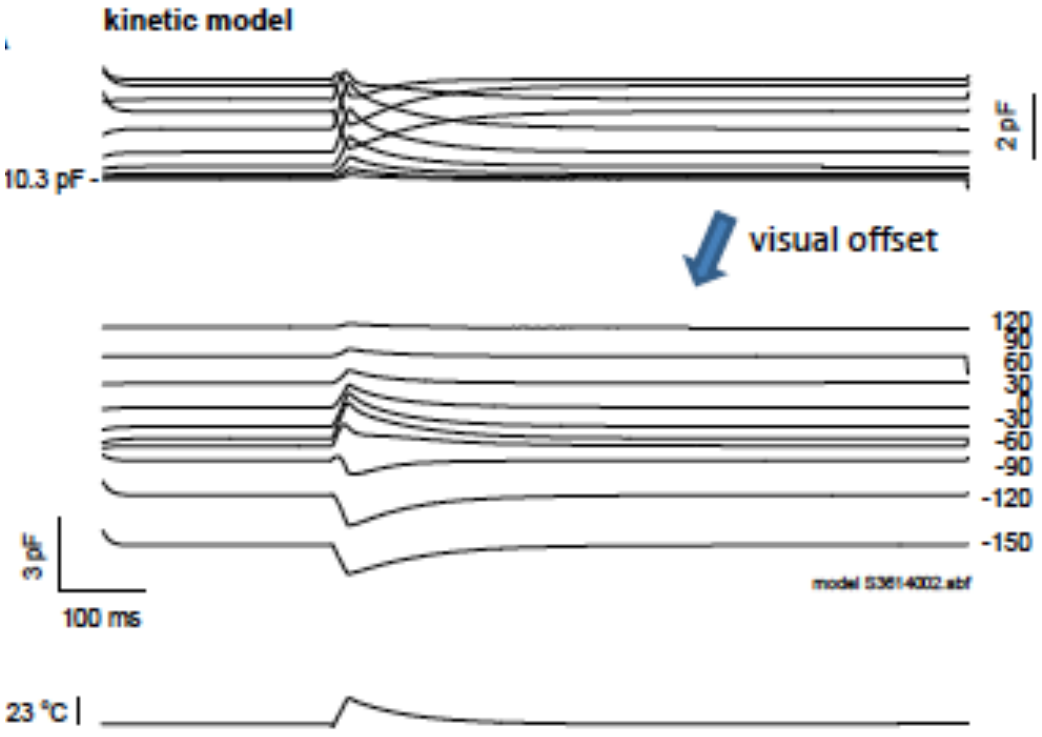

Figure 5 Kinetic model recapitulates biophysical data. Stimulation with the experimentally observed temperature change induced by an IR laser pulse induces C_m behavior similar to the biophysical results. Here the model transition rates are set to give a V_h of -71 mV.

Similar to the biophysical data, rapid temperature change followed by cooling induced characteristic changes in C_m, which derived from NLC magnitude and induced V_h shifts (**Fig. 5b,c**). As we deduced from the biophysical data, NLC V_h shifts directly mirror temperatures changes; in order to match the average biophysical data of 2.3V/s (about 20 mV/10^{O}C), an Arrhenius activation energy of 45 k J/mol was required. The model also recapitulates the reversal of ΔC_m near V_h (**Fig. 5d**). Also note that ΔCm recovers with temperature back to zero at voltages away from V_h, unlike the biophysical data (**Fig.4**), because the original model had no temperature sensitive linear C_m (**Fig. 5,** filled circles). However, by introducing a linearly temperature-dependent C_m, ΔC_m appears more similar to the biophysical data (**Fig. 5d**, open circles). The original implementation of the kinetic model [39] had temperature

dependence of both the backward intermediate rate, β, and the backward voltage-dependent rate, β. However, here better correspondence to the biophysical data was obtained by setting temperature dependence only in β.

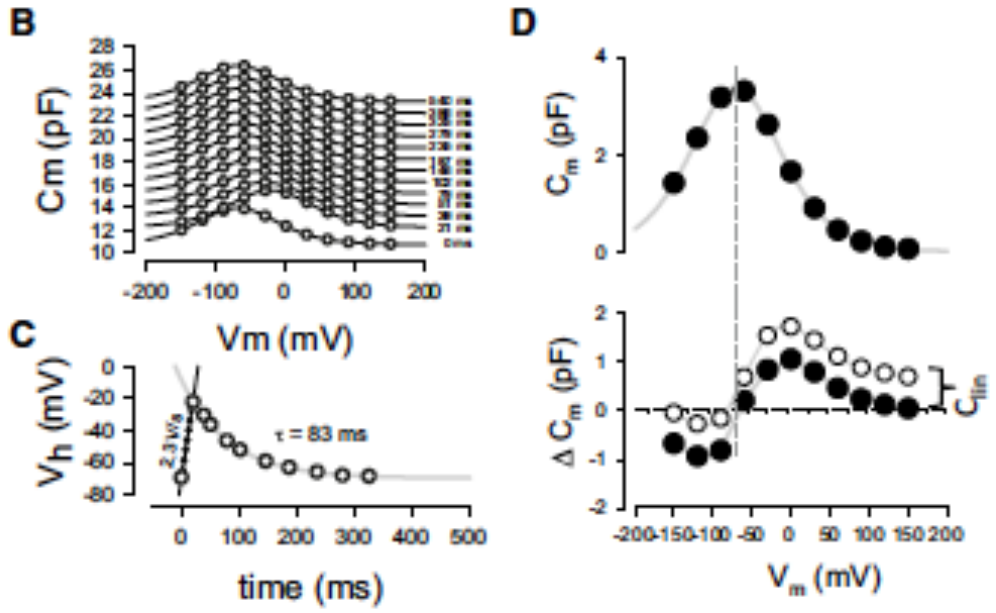

Figure 5B Plots of NLC showing rightward shifts along the voltage axis as a result of temperature increase. C**) Rates of V_h shift are comparable to biophysical data and directly follow temperature alterations.** D**) Voltage at reversal of ΔC_m is related to V_h. Note that ΔC_m goes back to zero, unlike the biophysical data, when C_{lin} is not temperature sensitive (closed circles). Including temperature dependence for C_{lin} results in an offset similar to the biophysical data (open circles, curly bracket).**

Current

We found two components of currents associated with fast temperature jump (**Fig. 6**). The first component was coincident with the IR heating phase, and its magnitude was related to the rate of heating (or correspondingly to the rate of linear C_m change) (**Fig. 6a, b**). This current appeared to reverse at positive voltages, as found by Shapiro et al.[28] (**Fig. 6c**). We agree with discussion on the matter, especially their interpretation that this may arise from asymmetrical fixed charges on the membrane

leaflets. The second slower component, which reversed near 0 mV, peaked at maximal temperature and then decayed during the cooling phase (**Fig. 6c, d**). We interpret this as an ionic current which is nonspecific with a reversal potential near zero. Sometimes we found that the second slow component obscured the first component as in Shapiro

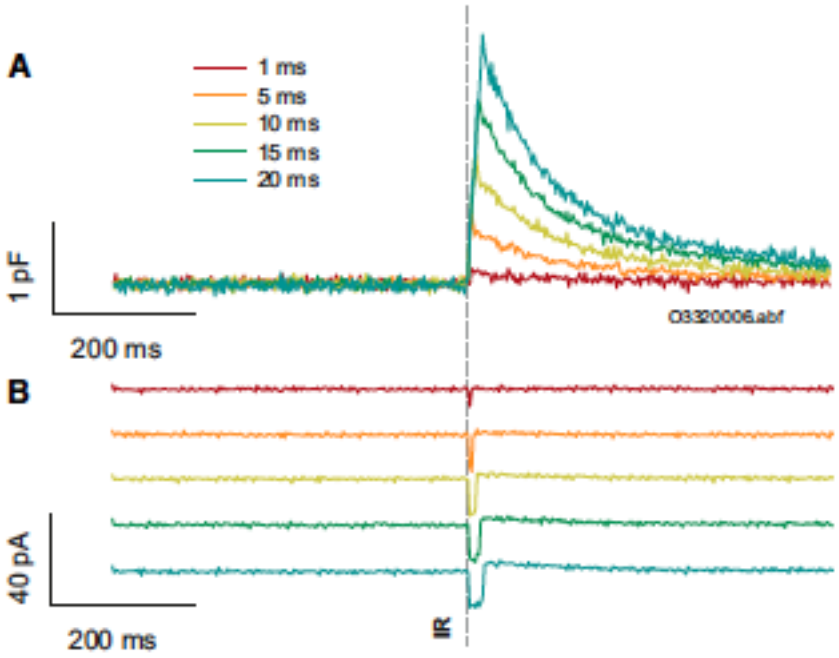

Figure 6 Two components of current induced during temperature jump. A) **Capacitance increases during temporally incremental IR laser pulses and** B) **corresponding currents arise. Current magnitude depends on rate of C_m change and duration depends on pulse duration. For all traces, pulses were delivered at a holding potential of 0 mV**

et al.[28]. Nevertheless, the rapid component is clearly observable in the traces near zero potential (**Fig. 6c**). The second slow decaying membrane current displays nonlinear features (**Fig. 6d**) reminiscent of G_{metL}, a conductance found in OHCs having marked

temperature dependence [30,42].

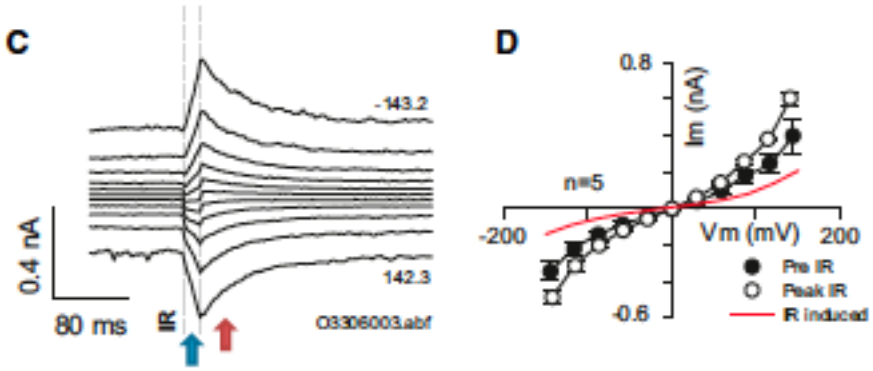

Figure 6C Current responses for a 20 ms duration pulse within the holding potential extremes indicated, stepped nominally at 30 mV. Note fast inward current response during the laser pulse, with a reversal potential predicted to be at positive potentials. Simultaneously, a slow decaying current with reversal near 0 mV is observed. The red arrow shows the sum of the two components (note step behavior around zero potential that rides on the slower current ramp) and the blue arrow shows the slow component after the fast component ends following the laser pulse. D) IV plot of average cell currents before and at termination of IR pulse (mean +/- se; n=5). Red line is IR induced current.

The current increase due to IR stimulation is likewise nonlinear, therefore unlikely due to linear decreases in R_S with temperature.

Discussion

Control HEK cells and HEK cells expressing the voltage-dependent protein SLC26a5 show very fast changes in membrane capacitance when rapid temperature jumps are delivered to the cells by IR laser. For control cells, rapid alterations in linear C_m directly follow changes in temperature as observed by Shapiro et al[28]; with the pulse energies we used, rates of change were up to 50 pF/s, and magnitudes peaked near 10% of the cell's resting membrane capacitance. Effects were reversible upon heat dissipation through the bathing solution. HEK cells expressing prestin showed additional effects on the Boltzmann characteristics of voltage sensor-related NLC. With 20 ms IR pulse durations, V_h was shifted in the positive direction at an

average rate of 2.3 V/s, corresponding to 20 mV/^{O}C, and subsequently returned to prior conditions as heat dissipated. In two cells, delivery of near maximum laser power produced V_h shift rates of 13-14 V/s. The rates of recovery of linear C_m and V_h with cooling were indistinguishable, indicating each is directly coupled to thermal energy. A simple kinetic model of prestin[39], possessing temperature sensitive, voltage-dependent transitions that move prestin into the expanded state, can mimic our biophysical observations. Thus, we conclude that temperature-induced alteration of transition rates between voltage dependent conformations of prestin can alter NLC as fast as thermal influences on the membrane double layer[28].

Capacitance

It is well established that capacitance is temperature sensitive, Taylor and Chandler having reported that squid axon capacitance increased 1% per degree centigrade[43]. Others have reported that the kinetics of voltage dependent channels is temperature sensitive, consequently influencing gating currents[29, 33], and necessarily altering their equivalent voltage-dependent capacitance. It is therefore not surprising that prestin-derived nonlinear capacitance is temperature dependent, as we have previously shown with slow alterations in bath temperature[23, 24]. Prestin's NLC V_h shifts about 20 mV per 10^{O}C. What may appear surprising is that prestin can redistribute between expanded and contracted states so rapidly upon infrared laser stimulation, showing V_h shift rates up to 14 V/s. Of course, by nature prestin is poised to transition between states at kilohertz rates, apparently capable of

rapidly responding to a variety of energy forms, including mechanical, electrical and thermal [8, 18, 22, 44]. Nevertheless, our observations are not simply related to the ability of prestin to rapidly transition between states, but more importantly about the efficacy in realigning the protein's operating voltage range by external influences, namely adjusting the gain of cochlear amplification.

Our modeling of temperature effects on prestin's voltage-dependent backward rate is similar to that employed to understand TRP channel heat sensitivity[31]. In this regard, we recently found that prestin is sensitive to capsaicin[45], an agent that mimics heat activation of TRP channels. However, in prestin the mechanism of action must be different than that of temperature, since it causes negative shifts in V_h, pointing towards action on forward rates. Thus, it will be of interest to evaluate the simultaneous effects of capsaicin and temperature on prestin NLC. Of course, other proposed mechanisms in TRP channels that may also contribute to temperature sensing by prestin, include allosteric mechanisms [46] and changes in specific heat capacity[47]. Nevertheless, the simplest scheme is likely that of temperature sensitive transition rates as we have modeled, which shows excellent agreement with the biophysical data. This is not to say that sensitivities of the other transitions in the model, namely, those displaying tension and chloride sensitivity cannot influence the temperature sensitive, voltage-dependent transition, as it is well known that a voltage-independent transition can affect the characteristics of a linked voltage-dependent one[48-50].

Currents

In this study, we used blockers to reduce ionic conductances so that capacitance could be effectively measured. We identified two components of residual current, one that is fast, being coincident with the duration of laser heating and one that follows bath temperature as it cooled. This observation is similar to that of Parker[33], who suggested that the fast component represented gating currents of oocyte ion channels. This was suggested because in the absence of the slow component, namely at its reversal potential, transient capacitive-like currents were revealed. While we do expect that sensor charge movement, namely gating-like currents, should arise when prestin's V_h suddenly shifts, we find no evidence of transient like currents near the reversal potential of our slow component, around 0 mV. We should note that when holding the cell at 0 mV we are interrogating a linear region of C_m, since NLC V_h is very negative. Our laser induced currents at 0 mV resemble those found by Shapiro et al[28], and we conclude that they represent currents generated by rapid changes in linear C_m. The second component of current which reverses near zero has some nonlinear features of a conductance, G_{metL}, found in OHCs [30,42]. Notably, increases in temperature augment the nonlinear current, and are not simply leakage currents.

Future Directions

Our study confirms that prestin derived nonlinear capacitance is vulnerable to rapid pertubations in biophysical conditions. We find that transitional changes in

prestin's motor conformation can induce large alterations in membrane capacitance that supplement other known linear effects[28]. Study strengths include our use of a well-established tet-inducible cell line, which highly expresses prestin. Although peak NLC and electromotile force generated by prestin-transfected cells is diminished compared to animal outer hair cells[15], various studies confirm that the use of a cell line is valid model for understanding the kinetics of prestin's function[37]. While our temperature jump protocol comprehensively examined membrane capacitance at voltages on either side of the peak NLC, it is also possible that this protocol was potentially damaging to the membranes of individual cells and introduced leak currents. Given some of the technical challenges of patching individual cells and subjecting them to harsh environmental changes, our study is also limited by a small sample size. We find that at maximal infrared laser stimulation, HEK cells expressing the voltage-dependent protein SLC26a5 redistribute between expanded and contracted states so rapidly, showing V_h shift rates up to 14 V/s. We were unable to substantiate definitively owing to technical difficulties and potential damage to individual cells, whether this value represents the upper limit of prestin's ability to move charge under rapid changes in biophysical conditions. We were also unable to conclusively characterize how membrane capacitance changes at voltages corresponding to V_h where NLC peaks. Future studies should interrogate cells for the voltage corresponding to the peak of NLC and carefully determine how the membrane capacitance of cells expressing prestin responds to increasing infrared laser stimulation when held at V_h.

We have previously determined that rapid changes in intracellular pressure, negative holding potential as well as changes in temperature results in shifts in the nonlinear capacitance function overtime. It is unclear however how these effects interact when coupled to rapid changes in thermal energy or if the interaction should be expected to be synergistic. Elucidating the effect of simultaneous changes in these biophysical properties will increase our understanding of how prestin's function is modulated in vivo.

Our study captures changes in membrane capacitance in HEK cells expressing prestin in a time window 24 to 72 hours post-transfection. Although our results were duplicable across the wide range of time to maturity of prestin trafficking, future studies should address how sensitivity to changes in temperature develops as a function of time after induction. Furthermore, results in HEK cells expressing voltage-dependent protein SLC26a5 should be compared to postnatal animal outer hair cells.

In summary, we find that SLC26a5 (prestin) is remarkably responsive to fast temperature jump, rapidly moving its operating point along the voltage axis. This susceptibility to thermal perturbations likely arises from the protein's natural ability to follow voltage changes at acoustic frequencies, but has implications for manipulation of cochlear amplifier gain control, as well. Thus, we predict that we may be able to drive auditory sensation by stimulation of OHCs with high frequency gated IR laser, and manipulate cochlear amplification *in vivo*.

References

1. Ashmore J, Avan P, Brownell WE, et al. The remarkable cochlear amplifier. Hear Res 2010;266:1-17.
2. Dallos P, Santos-Sacchi J, Flock A. Intracellular recordings from cochlear outer hair cells. Science 1982;218:582-4.
3. Brownell WE, Bader CR, Bertrand D, de Ribaupierre Y. Evoked mechanical responses of isolated cochlear outer hair cells. Science 1985;227:194-6.
4. Kachar B, Brownell WE, Altschuler R, Fex J. Electrokinetic shape changes of cochlear outer hair cells. Nature 1986;322:365-8.
5. Santos-Sacchi J, Dilger JP. Whole cell currents and mechanical responses of isolated outer hair cells. Hear Res 1988;35:143-50.
6. Santos-Sacchi J. On the frequency limit and phase of outer hair cell motility: effects of the membrane filter. J Neurosci 1992;12:1906-16.
7. Dallos P, Evans BN. High-frequency motility of outer hair cells and the cochlear amplifier. Science 1995;267:2006-9.
8. Frank G, Hemmert W, Gummer AW. Limiting dynamics of high-frequency electromechanical transduction of outer hair cells. Proc Natl Acad Sci U S A 1999;96:4420-5.
9. Kalinec F, Holley MC, Iwasa KH, Lim DJ, Kachar B. A membrane-based force generation mechanism in auditory sensory cells. Proc Natl Acad Sci U S A 1992;89:8671-5.
10. Huang G, Santos-Sacchi J. Mapping the distribution of the outer hair cell motility voltage sensor by electrical amputation. Biophys J 1993;65:2228-36.
11. Iwasa KH. A membrane motor model for the fast motility of the outer hair cell. J Acoust Soc Am 1994;96:2216-24.
12. Santos-Sacchi J, Navarrete E. Voltage-dependent changes in specific membrane capacitance caused by prestin, the outer hair cell lateral membrane motor. Pflugers Arch 2002;444:99-106.
13. Zheng J, Shen W, He DZ, Long KB, Madison LD, Dallos P. Prestin is the motor protein of cochlear outer hair cells. Nature 2000;405:149-55.
14. Santos-Sacchi J. Reversible inhibition of voltage-dependent outer hair cell motility and capacitance. J Neurosci 1991;11:3096-110.
15. Santos-Sacchi J, Shen W, Zheng J, Dallos P. Effects of membrane potential and tension on prestin, the outer hair cell lateral membrane motor protein. J Physiol 2001;531:661-6.
16. Ashmore JF. A fast motile response in guinea-pig outer hair cells: the cellular basis of the cochlear amplifier. J Physiol 1987;388:323-47.
17. Iwasa KH. Effect of stress on the membrane capacitance of the auditory outer hair cell. Biophys J 1993;65:492-8.
18. Gale JE, Ashmore JF. Charge displacement induced by rapid stretch in the basolateral membrane of the guinea-pig outer hair cell. Proc Biol Sci 1994;255:243-9.

19. Kakehata S, Santos-Sacchi J. Membrane tension directly shifts voltage dependence of outer hair cell motility and associated gating charge. Biophys J 1995;68:2190-7.
20. Ludwig J, Oliver D, Frank G, Klöcker N, Gummer AW, Fakler B. Reciprocal electromechanical properties of rat prestin: the motor molecule from rat outer hair cells. Proc Natl Acad Sci U S A 2001;98:4178-83.
21. Santos-Sacchi J, Kakehata S, Takahashi S. Effects of membrane potential on the voltage dependence of motility-related charge in outer hair cells of the guinea-pig. J Physiol 1998;510 (Pt 1):225-35.
22. Santos-Sacchi J, Song, L., Li, X.T. Firing up the Amplifier: Temperature, Pressure and Voltage Jump Studies on OHC Motor Capacitance. In: Cooper NPaK, David T., editor. Proceedings of 10th International Workshop on the Mechanics of Hearing; 2008; Keele University, Staffordshire, UK. p. 363-70.
23. Santos-Sacchi J, Huang G. Temperature dependence of outer hair cell nonlinear capacitance. Hear Res 1998;116:99-106.
24. Meltzer J, Santos-Sacchi J. Temperature dependence of non-linear capacitance in human embryonic kidney cells transfected with prestin, the outer hair cell motor protein. Neurosci Lett 2001;313:141-4.
25. Liberman MC, Gao J, He DZ, Wu X, Jia S, Zuo J. Prestin is required for electromotility of the outer hair cell and for the cochlear amplifier. Nature 2002;419:300-4.
26. Cheatham MA, Huynh KH, Gao J, Zuo J, Dallos P. Cochlear function in Prestin knockout mice. J Physiol 2004;560:821-30.
27. Yao J, Liu B, Qin F. Rapid temperature jump by infrared diode laser irradiation for patch-clamp studies. Biophys J 2009;96:3611-9.
28. Shapiro MG, Homma K, Villarreal S, Richter CP, Bezanilla F. Infrared light excites cells by changing their electrical capacitance. Nat Commun 2012;3:736.
29. Collins CA, Rojas E. Temperature dependence of the sodium channel gating kinetics in the node of Ranvier. Q J Exp Physiol 1982;67:41-55.
30. Santos-Sacchi J, Rybalchenko V, Bai JP, Song L, Navaratnam D. On the temperature and tension dependence of the outer hair cell lateral membrane conductance GmetL and its relation to prestin. Pflugers Arch 2006;452:283-9.
31. Voets T, Droogmans G, Wissenbach U, Janssens A, Flockerzi V, Nilius B. The principle of temperature-dependent gating in cold- and heat-sensitive TRP channels. Nature 2004;430:748-54.
32. Jia Z, Ling J, Gu JG. Temperature dependence of rapidly adapting mechanically activated currents in rat dorsal root ganglion neurons. Neurosci Lett 2012;522:79-84.
33. Parker I. Ionic and charge-displacement currents evoked by temperature jumps in Xenopus oocytes. Proc R Soc Lond B Biol Sci 1989;237:379-87.
34. Oliver D, He DZ, Klöcker N, et al. Intracellular anions as the voltage sensor of prestin, the outer hair cell motor protein. Science 2001;292:2340-3.
35. Abe T, Kakehata S, Kitani R, et al. Developmental expression of the outer hair cell motor prestin in the mouse. J Membr Biol 2007;215:49-56.

36. Bian SM, Koo, B.W., Kelleher, S., Santos-Sacchi, J., Navaratnam, D. Evaluating Prestin's Changing Biophysical Attributes in Development Using a Tet-Induced Cell Line. Proceedings of the 11th International Mechanics of Hearing Workshop: American Institute of Physics. p. 143-7.
37. Bian S, Koo BW, Kelleher S, Santos-Sacchi J, Navaratnam DS. A highly expressing Tet-inducible cell line recapitulates in situ developmental changes in prestin's Boltzmann characteristics and reveals early maturational events. Am J Physiol Cell Physiol 2010;299:C828-35.
38. Santos-Sacchi J. Determination of cell capacitance using the exact empirical solution of partial differential Y/partial differential Cm and its phase angle. Biophys J 2004;87:714-27.
39. Song L, Santos-Sacchi J. Disparities in voltage-sensor charge and electromotility imply slow chloride-driven state transitions in the solute carrier SLC26a5. Proc Natl Acad Sci U S A 2013;110:3883-8.
40. Kakehata, S., and J. Santos-Sacchi. 1996. Effects of salicylate and lanthanides on outer hair cell motility and associated gating charge. J.Neurosci. 16:4881-4889.
41. Tunstall, M. J., J. E. Gale, and J. F. Ashmore. 1995. Action of salicylate on membrane capacitance of outer hair cells from the guinea-pig cochlea. J.Physiol 485 (Pt 3):739-752.
42. Rybalchenko, V., and J. Santos-Sacchi. 2003. Cl- flux through a non-selective, stretch-sensitive conductance influences the outer hair cell motor of the guinea-pig. J.Physiol 547:873-891.
43. Taylor, R. E. 1965. Impedance of the squid axon membrane. Journal of Cellular and Comparative Physiology 66:21-25.
44. Santos-Sacchi, J. 1992. On the frequency limit and phase of outer hair cell motility: effects of the membrane filter. J.Neurosci. 12:1906-1916.
45. Wu, T., L. Song, X. Shi, Z. Jiang, J. Santos-Sacchi, and A. L. Nuttall. 2011. Effect of capsaicin on potassium conductance and electromotility of the guinea pig outer hair cell. Hear.Res. 272:117-124.
46. Jara-Oseguera, A., and L. D. Islas. 2013. The Role of Allosteric Coupling on Thermal Activation of Thermo-TRP Channels. Biophys J 104:2160-2169.
47. Clapham, D. E., and C. Miller. 2011. A thermodynamic framework for understanding temperature sensing by transient receptor potential (TRP) channels. Proc Natl Acad Sci U S A 108:19492-19497
48. Lacroix, J. J., A. J. Labro, and F. Bezanilla. 2011. Properties of deactivation gating currents in Shaker channels. Biophys.J. 100:L28-L30.
49. Colquhoun, D. 1998. Binding, gating, affinity and efficacy: the interpretation of structure-activity relationships for agonists and of the effects of mutating receptors. Br.J.Pharmacol. 125:924-947.
50. Shirokov, R. 2011. What's in gating currents? Going beyond the voltage sensor movement. Biophys.J. 101:512-514.